

X-ray Lines in Gamma-ray Bursts and Cerenkov Line Mechanism

Wei Wang

*National Astronomical Observatories, Chinese Academy of Sciences, Beijing
100012, China*

*Department of Physics, University of Hong Kong, Pokfulam Road, Hong Kong
wwang@bohr.physics.hku.hk*

May 20, 2004

Abstract. X-ray emission and absorption features are of great importance in our understanding the nature and environment of gamma-ray bursts (GRBs). So far, iron emission lines have been detected in at least four GRB afterglows. In this paper, the observational properties and physical constraints on materials surrounding GRB sources are reviewed, and several classes of theoretical models are also discussed. We will specially concentrate on the Cerenkov line mechanism, in which the broad iron lines are expected, and a small mass of Fe is required to produce the large line luminosity. In addition, our interpretation can favor the recent jet unified model for different classes of gamma-ray bursts with a standard energy reservoir.

Keywords: gamma-rays: bursts, X-rays, lines, radiation mechanism: nonthermal

1. X-ray lines in gamma-ray bursts

The detection of X-ray emission lines and absorption features in the GRB afterglows provides a powerful tool to probe the environments around GRB sources, and then probably gives us clues to the nature of the progenitors. Moreover, the identification of X-ray lines by the high spectral resolution detectors could directly provide the redshift information for GRBs.

Recent GRB observational reports have shown the emission line features in the X-ray afterglows of at least four GRBs (GRB 970508, Piro et al. 1999; GRB 970828, Yoshida et al. 1999; GRB 991216, Piro et al. 2000; GRB 000214, Antonelli et al. 2000). These lines generally last half day to several days, with large line width and very high line luminosity. The properties of the detected emission lines in GRBs are summarized in Table 1. The X-ray prompt emission is also detected in GRB 990712 with BeppoSAX (Frontera et al. 2001), which could be interpreted as either a line profile with centroid energy of 4.5 keV or a blackbody spectrum with the temperature ~ 1.3 keV, so we will not discuss it further in this paper. According to the variability and very large flux and equivalent width, we can estimate that there are large iron masses of 0.01 - $1.0M_{\odot}$ in the emission region with a size of $\sim 10^{15-16}$ cm if these



© 2018 Kluwer Academic Publishers. Printed in the Netherlands.

lines are supposed to be produced by fluorescence or recombination. So much Fe would come from the surrounding medium rather than GRB progenitors themselves, because it will involve the famous problem of baryon contamination.

A large number of irons in the close environment of GRBs imply the metal enriched process before GRBs occur. Then there exists a very dense medium surrounding the GRB progenitor, so we expect that the absorption features should be detected too. Up to now, only a discovery of a transient absorption edge in X-ray spectrum of GRB 990705 (Amati et al. 2000) has been reported. The absorption feature shows that the iron abundance is about 75 times higher than the solar value. Other ion emission lines were also detected in GRB 011211 by an XMM-Newton observation (Reeves et al. 2002). The X-ray spectrum reveals evidence for emission lines of Mg, Si, S, Ar, Ca and possible Ni. The line identification show the redshift $z = 1.88 \pm 0.06$, differing significantly from the known GRB redshift $z = 2.140 \pm 0.001$ by the spectroscopy of the optical afterglow (Holland et al. 2002), implying an outflow velocity for the line emitting material of $v = 25800 \text{ km s}^{-1}$ or $v/c = 0.086$. Additional evidence for the presence of ion lines were also suggested for two XMM-Newton spectra of GRB 001025A and GRB 010220 (Watson et al. 2002). These ion lines are attributed to the emission from the ionized optically thin plasma, indicating that thermal emission from light elements may be common in the early X-ray afterglows. And metal enrichments may occur preceding the GRB events.

2. Model constraints from observations

The iron line observations show constraints on the theoretical models: (1) If the iron lines are produced by fluorescence or recombination, we require that the compact regions ($\sim 10^{15-16} \text{ cm}$) contain $0.01 - 1M_{\odot}$ Fe with the electron density larger than 10^{10} cm^{-2} , but must be optically thin to electron scattering (size problem). (2) So much iron (corresponding to several solar mass material) cannot be produced by burst itself because of the famous problem of baryon contamination. These irons should come from the surrounding medium. Furthermore, iron-rich medium may be not consistent with the normal interstellar medium even in the dense region of stellar formation. (3) If we interpret the line width as due to the velocity of a supernova remnant, their sizes allow us to estimate the age of SNR which turn out to be tens of days, while at this time, cobalt nuclei would dominate and the line would be produced mainly by cobalt not iron (kinematic problem).

A large mass of Fe around the progenitor really produces a challenge to the present GRB models. And the problem also focuses on how the torus of iron-rich material formed. Mészáros & Rees (1998) have shown that the circumburst environment created by the stellar wind before the hypernova (Paczynski 1998). While, this scenario may not produce so high luminosity Fe lines. Recently, Dado, Dar & De Rújula (2003) argued that the line detected are not the real iron lines but the strongly Doppler-blueshift Ly α line emissions by jets of highly relativistic cannonballs produced by a supernova. At present, there are mainly two classes of model put forward to explain the lines: the geometry dominated and engine dominated models, and the key difference is the reason for the observed duration of the line emission.

In the geometry dominated models, the line emission duration is due to light travel time effect. Since the lines appear in the timescale of one day, the emission size estimated is about 10^{16} cm. A favorable situation is expected in the supranova (Vietri & Stella 1998), where a GRB is preceded by a supernova explosion for several months to years with ejection of an iron-rich massive shell. In this scenario, high density in excess of 10^{10}cm^{-3} may be expected, and Fe absorption features of strength comparable to these in emission should be also be detected. While, in the engine dominated models, the emission material, at a typical emission size about 10^{13} cm, can be pre-GRB ejecta or the expanding envelope of a supergiant GRB progenitor (Rees & Mészáros 2000, Mészáros & Rees 2001). They have argued that the strong line emission can be attributed to the interaction of a continuing post-burst relativistic outflow from the central decaying magnatar with the progenitor stellar envelope at distance less a light hour, and only a small mass Fe is required.

3. Cerenkov line mechanism

We have proposed a new mechanism Cerenkov line emission for the lines in X-ray afterglows. (Wang, Zhao & You 2002). As we know, Cerenkov radiation is produced when the particle velocity exceeds the light speed in the medium. Furthermore, You & Chen (1980) argued that for relativistic electrons moving through a dense gas, the Cerenkov effect will produce peculiar atomic/molecular emission lines: Cerenkov lines. They also extended the work to the X-ray band, such as Fe $K\alpha$ lines (You et al. 2000). Cerenkov line emission has following remarkable features (see Fig. 1): broad, asymmetrical, Cerenkov redshift and polarized if relativistic electrons have an anisotropic velocity distribution.

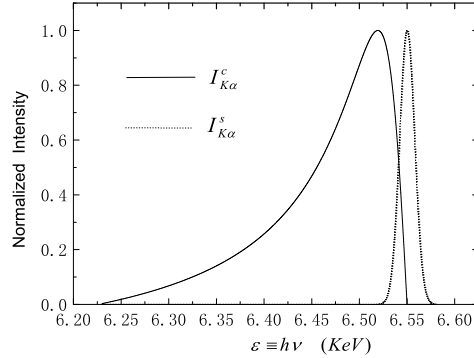


Figure 1. The calculated profile of Cerenkov line $I_{K\alpha}^c \sim \varepsilon$ of iron ion Fe^{+21} in optically thick case, where $\varepsilon \equiv h\nu$ is the energy of line photon (You et al. 2003). The Cerenkov line-profile is broad, asymmetric, and redshifted. The profile of a normal line by spontaneous transition $I_{K\alpha}^s \sim \varepsilon$ is also plotted for the comparison.

Here, we emphasize the special importance of the Cerenkov redshift which markedly strengthens the emergent intensity of the Cerenkov emission line. For an optically thick dense gas, the emergent line is determined both by the emission and absorption. The absorption mechanisms for the normal line and Cerenkov line are extremely different. The intensity of normal line, I^n is greatly weakened by the strong resonant absorption $k_{lu}(\nu_{lu})$ (the subscripts u and l denote the upper and lower-levels) due to the fact that the normal line is located exactly at the position of the intrinsic frequency ν_{lu} where k_{lu} is very large. In the extreme case of a very dense gas, the emergent flux has the continuum with a black body spectrum, and the normal line disappeared, $I^n \sim 0$. However, the Cerenkov line, located at $\nu < \nu_{lu}$ due to the redshift, can avoid the resonant absorption because of $k_{lu}(\nu < \nu_{lu}) \rightarrow 0$ (see the special dispersion relations at a wavelength shown in Fig. 2). The main absorption mechanism which affects the intensity of Cerenkov line is the photoionization absorption k_{bf} which is very small compared with k_{lu} . Thus the Cerenkov line photons can easily escape from deep inside a dense gas cloud, causing a strong emergent line flux, only if the density of relativistic electrons N_e is high enough. In other words, the dense gas appears to be more transparent for the Cerenkov line than normal line, which makes it possible for the Cerenkov line mechanism to dominate over the normal line mechanisms when the gas is very dense and there exist abundant relativistic electrons in the emission region.

In the astrophysical processes of GRBs, a large amount of relativistic electrons and dense gas regions could exist. For the long burst after-

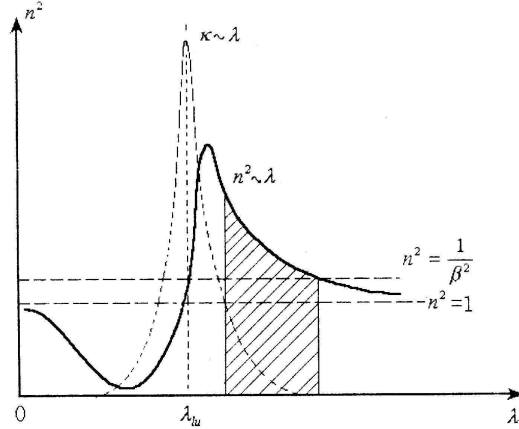


Figure 2. The relations between refractive index n^2 which is proportional to emissivity and wavelength λ , and between extinction coefficient κ and λ . The Cerenkov radiation survives in the shaded narrow region (You et al. 2000).

glows localized so far, the host galaxies show signs of star formation activity, where the high-density environment is expected. Recent broadband observations of the afterglows of GRB 000926 (Piro et al. 2001) and statistical analysis (Reichart & Price 2002) imply the evidence for a fireball in a dense medium. When the ultra-relativistic blast waves interact with the dense regions, very strong Cerenkov line emission in X-ray band would be observed, and Cerenkov mechanism may dominate in the case of the optically thick gases. Importantly, broad line features are naturally explained in our model (see Fig. 1).

The total intensity of Cerenkov line is (You et al. 2000)

$$I^c = Y \left[\ln(1 + X^2) + 2 \left(1 - \frac{\arctan X}{X} \right) \right], \quad (1)$$

where $Y \equiv \frac{N_e C_1}{2 k_{bf}}$, and $X \equiv \sqrt{\frac{k_{bf}}{C_2}} y_{lim}$, N_e is the relativistic electron density, $y_{lim} = C_0 \gamma_0^2$, γ_c is the electron Lorentz factor, and

$$\begin{aligned} C_0 &= 1.05 \times 10^{-76} \varepsilon_{lu}^{-4} A_{ul} g_u N_{Fe} \frac{S_l}{g_l}, \\ C_1 &= 5.77 \times 10^{-53} \varepsilon_{lu}^{-2} A_{ul} g_u N_{Fe} \frac{S_l}{g_l}, \\ C_2 &= 1.75 \times 10^{-87} \varepsilon_{lu}^{-4} \Gamma_{lu} A_{ul} g_u N_{Fe} \frac{S_l}{g_l}, \\ k_{bf} &= 8.4 \times 10^{-46} \varepsilon_{lu}^{-3} N_{Fe} S_2. \end{aligned} \quad (2)$$

The damping constant Γ_{lu} is related to Einstein's coefficient A_{ul} , g_u is the statistical weights. For Fe $K\alpha$ line, $\varepsilon_{lu} = 6.4$ keV, only levels

$l = 1, u = 2$ are considered, and $S_1 = g_1 = 2, g_2 = 8$, and $S_2 \sim 5$ for the GRB afterglow.

In the optically thick gas, we have found $X \gg 1$, then we can simplify the formulae of Cerenkov line intensity as $I^c \simeq 2Y(\ln X - 1)$ (Wang, Zhao & You 2002). And we only take the main contribution $2Y$ in our following estimation, so

$$I^c \sim \frac{C_1}{k_{bf}} N_e \sim 1.12 \times 10^{-7} \varepsilon_{12} A_{21} N_e. \quad (3)$$

For the optically thick case, the outward flux per unit area and per unit time $\pi F \approx \pi I^c$. Assuming that there exist a lot of spherical clouds with dense gas that is distributed homogeneously in the circumburst environment, the cloud radius and number are R, N_c respectively, an isotropic fireball interacts with these clouds. Therefore, the total line luminosity from the clouds is $L^c = 4\pi^2 R^2 N_c I^c$. Defining a covering factor $C \equiv N_c \pi R^2 / 4\pi D^2$, where D is the distance between the clouds and burst center, then

$$L^c = 16\pi^2 C D^2 I^c \sim 8.2 \times 10^{32} C_{0.1} D_{16}^2 N_e \text{ erg s}^{-1}, \quad (4)$$

where we have taken $A_{21} = 4.6 \times 10^{14} \text{ s}^{-1}$ and the characteristic scales $C \sim 0.1, D \sim 10^{16} \text{ cm}$. From Eq. (4), we can clearly see that the total line luminosity by the Cerenkov mechanism is strongly dependent on the electron density rather than the iron abundance. Thus, we propose that some classes of GRB models predict the presence of a very high relativistic electron density, therefore the ultra-strong iron lines in the X-ray afterglows can be explained probably without additional request for initial and external conditions of iron-rich torus.

We also could estimate the relativistic electron density required for X-ray lines from four GRB afterglows. Take the cosmological model with $H_0 = 70 \text{ km s}^{-1} \text{ Mpc}^{-1}, \Omega_0 = 1/3, \Omega_\Lambda = 2/3$, and let $C_{0.1} = D_{16} = 1$, we find that the electron densities $N_e \sim 10^{10} - 10^{11} \text{ cm}^{-3}$ are similar to the one estimated by other models. We first simply estimate the relativistic electron density from the fireball, $N_e \sim E / 4\pi D^2 \Delta_D \gamma m_p c^2$, and taking the isotropic energy $E \sim 10^{53} \text{ erg}, \gamma \sim 100, \Delta_D \sim \gamma c T$ (T is the duration $\sim 10 \text{ s}$), we obtained the density $N_e \sim 10^8 \text{ cm}^{-3}$, which will be lower than our requirement in the model. So we think the relativistic electrons should come from other processes. We here propose that the electrons would be produced by a pulsar wind from the central millisecond magnetar (Thompson 1994) or e^+e^- outflow from the Kerr black hole with magnetized torus (MacFadyen & Woosley 1999) as the delayed injection after GRB events. Our interpretation is similar to that of Rees & Mészáros (2000), but we consider the e^+e^- outflow instead

of electromagnetic flux. The luminosity is required as high as $L \sim 4\pi D^2 N_e c \gamma_e m_e c^2 \sim 10^{48} \text{erg s}^{-1}$, where we take $N_e \sim 10^{10} \text{cm}^{-3}$, $\gamma_e \sim 10$ at the distance of 10^{16}cm . The luminosity could be satisfied by the central compact objects with the acceptable parameters such as very strong magnetic field. Because the scattering cross section of relativistic electrons will be near to the zero due to the Klein-Nishina formula at the very high frequency (due to the Doppler effect), we need not worry about the electron scattering process will greatly affect the line profile and intensity.

Furthermore, we also have considered the optically thin case for the Cerenkov line emission mechanism (Wang 2003). In this case, The emission intensity will be dependent on both the electron density and iron abundance (in a form $\propto X^2 Y$). Meanwhile, the computations show that only a small mass of iron about $10^{-6} M_\odot$ is needed to produce the high line luminosity within the emission region of $\sim 10^{16} \text{cm}$, so a normal homogeneous medium around the GRB progenitor could meet the requirement.

Finally, the research and development of thirty years on gamma ray bursts more and more make the astronomers believe that there probably exists a unified picture for gamma ray bursts. Recently, some researchers proposed the jet unified models of short and long gamma-ray bursts, X-ray rich gamma-ray bursts, and X-ray flashes (Lamb et al. 2004; Yamazaki et al. 2004). The jet models assume the different classes of gamma-ray bursts have a standard total energy within a range of $10^{50} - 10^{51} \text{erg}$ (Frail et al. 2001). However, the standard energy is much lower than the total energy limit determined from the X-ray emission lines, $\sim 10^{52} \text{erg}$ (Ghisellini et al. 2002). Since based on the fluorescence or recombination, the line radiation is isotropic, and the burst energy cannot be lower than the X-ray afterglow energy, so the inconsistency still exists. But the Cerenkov line mechanism has not the problem and could make the jet unified picture more convincible, because the Cerenkov line intensity can be independent of the prompt energy of gamma-ray bursts, and if the relativistic electrons distribute not in the homogeneous direction, the Cerenkov line emissions are not isotropic too, the “beaming” effect will decrease the total X-ray afterglow energy to the same order of the standard energy reservoir.

References

- Amati, L. et al. 2000, *Science*, 290, 953
 Antonelli, L.A. et al. 2000, *ApJ*, 545, L39
 Dado, S., Dar, A. and De Rújula, A. 2003, *ApJ*, 585, 890
 Djorgovski, S.G. et al. 2001, *ApJ*, 562, 654

Table I. The properties of X-ray emission lines in GRBs. Here the cosmological model $(\Omega_M, \Omega_\Lambda, h) = (1/3, 2/3, 0.7)$ is taken, the redshift of GRB 000214 is determined only based on Fe $K\alpha$ emission identification. Two lines is discovered in GRB 991216, generally, one is identified as the fluorescent line, the other as the recombination.

GRB	Detector	z	Line Energy keV	Width keV	Intensity $10^{-5} \text{ ph cm}^{-2}\text{s}^{-1}$	Line Luminosity erg s^{-1}	Reference
970508	BeppoSAX	0.835	3.4	≤ 0.5	5.0	2.7×10^{44}	1,2
970828	ASCA	0.957	5.04	0.31	1.9	1.1×10^{44}	3,4
991216	Chandra	1.02	3.49	0.23	3.2	4.0×10^{44}	5,6
			4.4	1.0	3.8	4.8×10^{44}	5
000214	BeppoSAX	0.47	4.7	0.2	0.9	4.0×10^{43}	7

References: 1. Piro et al. 1999; 2. Metzger et al. 1997; 3. Yoshida et al. 1999; 4. Djorgovski et al. 2001; 5. Piro et al. 2000; 6. Vreeswijk et al. 2000; 7. Antonelli et al. 2000.

- Frail, D.A. et al. 2001, ApJ, 562, L55
Frontera, F. et al. 2001, ApJ, 550, L47
Ghisellini, G. et al. 2002, A&A, 389, L33
Holland, S. et al. 2002, AJ, 124, 639
Lamb, D.Q., Donaghy, T.Q. & Graziani, C. 2004, New Astronomy, 48, 459
MacFadyen, A. and Woosley, S.E. 1999, ApJ, 524, 262
Mészáros, P. and Rees, M.J. 1998, MNRAS, 299, L10
Mészáros, P. and Rees, M.J. 2001, ApJ, 556, L37
Metzger, M.R. et al. 1997, Nature, 387, 878
Paczynski, B. 1998, ApJ, 494, L45
Piro, L. et al. 1999, ApJ, 514, L73
Piro, L. et al. 2000, Science, 290, 955
Piro, L. et al. 2001, ApJ, 558, 442
Rees, M.J. and Mészáros, P. 2000, ApJ, 545, L73
Reeves, J.N. et al. 2002, Nature, 416, 512
Reichart, D.E. and Price, P.A. 2002, ApJ, 565, 174
Thompson, C. 1994, MNRAS, 270, 480
Vietri, M. and Stella, L. 1998, ApJ, 507, L45
Vreeswijk, P.M. et al. 2000, GCN notice 496
Wang, W., Zhao, Y. and You, J.H. 2002, ApJ, 576, L37
Wang, W. 2003, the Master's Thesis, Chinese Academy of Sciences
Watson, D. et al. 2002, A&A, 393, L1
Yamazaki, R., Ioka, K. & Nakamura, T. 2004, ApJ, 607, L103
Yoshida, A. et al. 1999, A&AS, 138, 433
You, J.H. and Cheng, F.H. 1980, Acta Phys. Sinica, 29, 927
You, J.H. et al. 2000, A&A, 362, 762
You, J.H. et al. 2003, ApJ, 599, 164